Functional Immobilization of a DNA-Binding Protein at a Membrane Interface via Histidine Tag and Synthetic Chelator Lipids[†]

Christian Dietrich,[‡] Oliver Boscheinen,[§] Klaus-Dieter Scharf,[§] Lutz Schmitt,[‡] and Robert Tampé*[,‡,||]

Lehrstuhl für Biophysik E22, Physik Department, Technische Universität München, D-85478 Garching, Germany, Molekulare Zellbiologie, Universität Frankfurt, Marie-Curie Strasse 9, D-60439 Frankfurt/M, Germany, and Max-Planck-Institut für Biochemie, Am Klopferspitz 18a, D-82152 Martinsried, Germany

Received September 27, 1995; Revised Manuscript Received November 17, 1995[⊗]

ABSTRACT: The coupling of a DNA-binding protein to self-organized lipid monolayers is examined at the air−water interface by means of film balance techniques and epifluorescence microscopy. We used two recombinant species of the heat shock factor HSF24 which differ only in a carboxy-terminal histidine tag that interacts specifically with the nickel-chelating head group of a synthetic chelator lipid. As key function, HSF24 binds to DNA that contains heat-shock responsible promoter elements. In solution, DNA−protein complex formation is demonstrated for the wild type and fusion protein. Substantial questions of these studies are whether protein function is affected after adsorption to lipid layers and whether a specific docking via histidine tag to the chelator lipid leads to functional immobilization. Using lipid mixtures that allow a lateral organization of chelator lipids within the lipid film, specific binding and unspecific adsorption can be distinguished by pattern formation of DNA−protein complexes. At the lipid interface, functional DNA−protein complexes are only detected, when the histidine-tagged protein was immobilized specifically to a chelator lipid containing monolayer. These results demonstrate that the immobilization of histidine-tagged biomolecules to membranes via chelator lipids is a promising approach to achieve a highly defined deposition of these molecules at an interface maintaining their function.

Biofunctionalized interfaces are of special interest in life and material science, since they open a wide range of opportunities to mimic biological interfaces and to gain insights into molecular and cellular recognition processes. Technical applications such as biofunctionalization or biosensing are related to this topic. One of the key questions in this field is how to reach an effective and well-defined enrichment, immobilization, and orientation of biomolecules optimized for function and binding capacity at an interface. Unfortunately, proteins often unfold and denature at interfaces (Norde, 1986; Schmidt et al., 1990), which causes, for example, immune response against implants (Mulvihill et al., 1985). Furthermore, denatured proteins can promote protein adsorption and multilayer formation, reflecting a cooperative adsorption process.

Here, we used lipid monolayers spread at the air−water interface as a model system to investigate protein function at lipid interfaces. The high energy density of the air−water interface may cause unfolding of proteins (McRitchie, 1986; Graham & Phillips, 1978; Nitsch et al., 1990). To avoid such an unfavored process and to mimic cellular interfaces, a lipid layer can be deposited on the air−water interface (Dietrich et al., 1993). In addition, lipid films offer further advantages: (i) In aqueous solution, lipids form spontaneously lateral structures by self-assembly which can be transferred onto solid supports by various techniques [Tamm & McConnell, 1985; Kühner et al., 1994; Dietrich & Tampé (1995) and reviewed by Ulman (1991) and Tampé et al. (1995)]. (ii) The common membrane architecture made up by amphiphilic compounds tolerates the combination of a vast variety of natural and synthetic molecules, which built up functional units and modify layer composition and morphology (Martin et al., 1981; Tscharner et al., 1981; Lang et al., 1992; Spinke et al., 1992; Schmitt et al., 1994). (iii) Lipid films organize in two dimensions by phase separation or extrinsic forces (Lee et al., 1994; Dietrich & Tampé, 1995). Film balance techniques are well established to investigate the properties of lipid monolayers (Gains, 1966; Adamson, 1990).

In biochemistry and molecular biology, the expression of histidine-tagged fusion proteins is a well-established technique for identification, one-step purification, and characterization of gene products (Hochuli et al., 1988; Porath et al., 1976). This powerful technique is based on the affinity of amino- or carboxy-terminally-fused five to six histidine residues for metal chelate complexes, such as *N*-nitrilotriacetic acid (NTA) or imidodiacetic acid (IDA). Association and dissociation of the histidine-tagged protein can be triggered by competitors (e.g., histidine, imidazole), by shifting the pH value, or by loading or unloading the chelate complex.

We have combined this strategy with the properties of self-organizing systems by synthesis of various chelator lipids which harbor a nickel-chelating lipid head group (Schmitt et al., 1994). These lipids are highly sensitive toward nickel

[†] This work was supported by the Deutsche Forschungsgemeinschaft (Grant Scha 577/5-1 to K.-D.S. and Grant Ta157/1 to R.T.), by the Fonds der Chemischen Industrie (grant to K.-D.S.), and by the Bundesministerium für Bildung und Forschung (BMBF, Grant 0310253 A to K.-D.S. and Grant 0310851 to R.T.).

* Correspondence should be addressed to this author at the Max-Planck-Institut für Biochemie, Am Kopferspitz 18a, D-82152 Martinsried, Germany. Phone: ++49-89-8578-2646. Fax: ++49-89-8578-2641. E-mail: tampe@vms.biochem.mpg.de.

[‡] Technische Universität München.

[§] Universität Frankfurt.

[||] Max-Planck-Institut für Biochemie.

[⊗] Abstract published in *Advance ACS Abstracts,* January 15, 1996.

0006-2960/96/0435-1100$12.00/0

ions (Schmitt et al., 1994), and they specifically interact with histidine-tagged biomolecules (Dietrich et al., 1995; Gritsch et al., 1995). Furthermore, by phase segregation, histidine-tagged molecules can be organized laterally, forming two-dimensional arrays (Dietrich et al., 1995; Gritsch et al., 1995). In this study, we investigated the influence of protein immobilization via the specific binding to a chelator lipid on protein function and compared it with unspecific binding. Therefore, we prepared laterally structured lipid films which segregate into chelator lipid-rich domains. As chelator lipid, we used unloaded NTA−dioctadecylamine (NTA−DODA) or nickel-loaded Ni-NTA−DODA. The experiments were carried out with the heat shock transcription factor HSF24 from *Lycopersicon peruvianum* (tomato). HSF24 is a transcription activator, which by binding to heat-stress responsible promoter elements (HSE) promotes transcription of heat shock genes (Scharf et al., 1990, 1994; Treuter et al., 1993). The newly formed stress proteins are essential for cells to survive stress situations and to rapidly restore their normal pattern of activities (Nover, 1991; Scharf et al., 1994). Here, the effect of HSF24 immobilization to lipid films and its functional integrity is investigated. This concept might help to elaborate the structure of the protein−DNA complex by two-dimensional crystallization at chelator−lipid interfaces.

MATERIALS AND METHODS

Lipids. The chelator lipid (NTA−DODA) was synthesized and characterized as described (Schmitt et al., 1994). In brief, after addition of trimethylsilyl groups, the silylated N^{α}-Boc-L-lysine was coupled to the synthetic lipid dioctadecylamine (DODA) via succinic anhydride in organic solution using active ester chemistry. The protecting group (Boc) was cleaved by trifluoroacetic acid. Bromoacetic acid was added, yielding the NTA−chelator lipid (NTA−DODA). This product was characterized in detail by TLC, FTIR, and ^{1}H-NMR. Dimyristoyl-L-α-phosphatidylcholine (DMPC) was purchased from Avanti Polar Lipids (Birmingham, AL). TexasRed-labeled dipalmitoyl-L-α-phosphatidylethanolamine (TR-DPPE) was ordered from Molecular Probes (Eugene, OR). Organic solvents were purchased from Sigma (Deisenhofen, Germany). All lipids were used without further purification. Equimolar lipid mixtures of NTA−DODA/DMPC (10 nmol) were spread in chloroform/methanol (3/1, v/v) at the air−water interface. In the case of Ni-NTA−DODA, complex formation was achieved in the presence of a 5-fold molar excess of $NiCl_2$ in the spreading solution.

Expression and Purification of Recombinant HSF24. pJCHSF24HC was obtained by cloning an *Ecl*XI fragment coding for tomato Lp-HSF24 amino acid positions 1−294 from pHSF24 (Treuter et al., 1993) into *Eco*RI-digested pJC20HC after filling in overhanging ends with Klenow DNA polymerase. pJC20HC is a derivative of pJC20 (Clos et al., 1990) that allows the fusion of six histidine residues to the carboxy-terminal end of Lp-HSF24. To obtain recombinant Lp-HSF24 with six histidine residues tagged to the amino-terminal end, pHSF24HN was constructed by ligation of a *Nde*I−*Bam*HI fragment of pJCHSF24HC into 6His-pET11d. The fusion proteins were expressed in *E. coli* strain BL21DE3(pLys) as described by Studier et al. (1990). Soluble *E. coli* protein was dissolved in buffer containing 50 mM Tris/HCl, pH 7.5, 250 mM NaCl, 0.5 mM EDTA, 2.5 mM $MgCl_2$, 1 mM phenylmethanesulfonyl fluoride, and 5% glycerol. HSF24 was purified according to the manufacturer's protocol (Qiagen) using NTA−agarose as affinity matrix. The bound protein was eluted with 0.1 M imidazole and dialyzed against buffer A (10 mM HEPES, 100 mM NaCl, pH 7.5). The purification procedure was monitored by SDS−PAGE (Laemmli, 1970). The wild-type protein was obtained by removal of the amino-terminal histidine tag by thrombin (Sigma) cleavage.

DNA Gel Mobility Shift Assays. Formation of sequence-specific DNA−protein complexes was analyzed by electrophoretic DNA mobility shift assays. A modified protocol of Zimarino and Wu (1987) was used. The DNA-binding reaction was performed (20 min at room temperature) by mixing increasing molar ratios of recombinant proteins (0−4-fold excess) with 50 pmol of a double-stranded oligonucleotide (5′-GCCAGAAGCTTCTAGAAAGC-3′, HSE3) which contains three inverted repeats of the core motif, -AGAAN-, characteristic of all eukaryotic heat stress promoter elements (Nover, 1987; Xiao & Lis, 1988). One of the oligonucleotide strands was synthesized with a fluorescein molecule covalently bound to the 5′-end [dsHSE3 fluorescein-labeled top strand (FT)/nonlabeled bottom strand (NB)] to visualize free and bound oligonucleotides (at 320 nm) after separation on a 1% agarose gel in TAE buffer (40 mM Tris/acetate, 1 mM EDTA, pH 8.0). For competition experiments, a 3-fold or 6-fold molar excess (in relation to dsHSE3) of double-stranded oligonucleotides with the sequence given above or of a mutated oligonucleotide (5′-GCCATAAGCTTGTACAAAGC-3′) was added to the binding reaction together with fluorescein-labeled dsHSE3.

Film Balance Measurements. The film balance unit consists of an epifluorescence microscope placed on top of a Langmuir trough (30 mm × 220 mm) which carries a subphase volume of 30 mL containing buffer A (10 mM HEPES, 100 mM NaCl, pH 7.5). To achieve a homogeneous distribution, the fluorescence-labeled oligonucleotide (dsHSF3 FT/BN) was dissolved in buffer A, yielding a final concentration of 15 nM. After spreading of the lipid mixture (10 nmol), the lateral pressure was adjusted by variation of the surface area. The protein (1.5 nmol) was injected into the subphase via a small hole in the trough without touching and disturbing the air−water interface, yielding a final concentration of 45 nM. The surface tension was measured with a Wilhelmy system (accuracy ±0.1 mN/m). For exact temperature control (±0.2 °C), peltier elements were placed below the base-plate. The lipid monolayers were compressed with 3 Å^2/(molecule·min). Compression, expansion, surface tension, and temperature are computer-controlled. The lateral distribution of fluorescence-labeled lipids and oligonucleotides was imaged by means of a epifluorescence microscope which is mounted on a x-y translation stage. By changing adapted filters, the two fluorescence probes [fluorescein (F) and TexasRed (TR)] can be observed simultaneously. TR-DPPE stains the fluid, liquid-expanded (LE) phase of the lipid monolayer. Fluorescein labels the oligonucleotide and thereby DNA−protein complexes (see DNA Gel Mobility Shift Assays). The fluorescence is detected with a SIT-camera (Hamamatsu, Hamamatsu, Japan).

RESULTS

Recombinant Heat Shock Factor HSF24 Is Functional as Wild Type and Fusion Protein. As a model system to

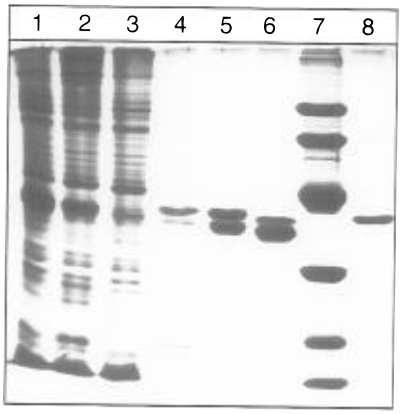

FIGURE 1: Expression and purification of HSF24. Coomassie-stained polyacrylamide gel (12%) demonstrating the expression and purification of amino-terminally histidine-tagged HSF24. Lane 1: *E. coli* cell lysate 3 h after induction with IPTG. Lane 2: Soluble fraction of the cell lysate before incubation with Ni-NTA−agarose beads. Lane 3: Nonbound protein. Lane 4: Wash fraction. Lane 5: Protein eluted with 0.1 M imidazole and dialyzed. Lane 6: HSF24 after thrombin cleavage. Lane 7: Protein marker (molecular masses: 94, 67, 43, 30, 20.1, and 14.4 kDa). Lane 8: Carboxy-terminally-tagged HSF24 expressed and purified as illustrated for the amino-terminally-tagged HSF24.

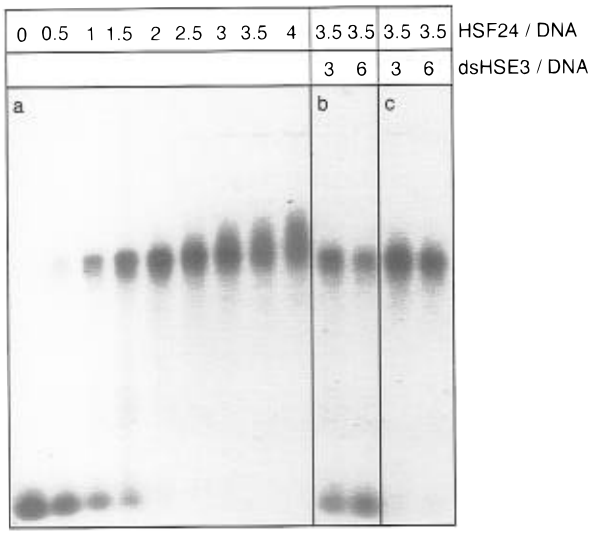

FIGURE 2: DNA gel mobility shift assay. (a) Fluorescence-labeled double-stranded oligonucleotides (50 pmol of dsHSE3 FT/NB) containing three heat shock elements (see Materials and Methods) were incubated with an increasing ratio of purified carboxy-terminally-tagged HSF24 (0−200 pmol). At a HSF24 to fluorescent dsHSE3 ratio of 3.5, DNA competition assays were performed in the presence of 150 or 300 pmol (3-fold or 6-fold molar excess) of the unlabeled dsHSE3 (b) and mutated oligonucleotide, respectively (c).

investigate protein function at lipid interfaces, we used two species of HSF24 (wild type and fusion protein) which differ only in the additional sequence of six histidines at the carboxy terminus. Therefore, amino- or carboxy-terminally-tagged histidine fusion proteins were expressed in *E. coli* and purified by immobilized metal affinity chromatography. The amino-terminal histidine tag was cleaved by thrombin treatment (Figure 1). To test the functional integrity of the heat shock factor, DNA mobility shift assays were performed (Figure 2). HSF24 specially binds to fluorescence-labeled oligonucleotides that contain three inverted repeats of heat shock responsible promoter elements (dsHSE3, see Materials and Methods). By adding HSF24, defined fluorescence-

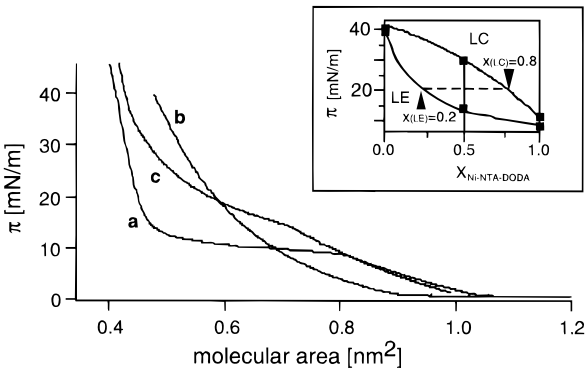

FIGURE 3: Phase behavior of lipid monolayers. Area−pressure isotherms of Ni-NTA−DODA (a), DMPC (b), or Ni-NTA−DODA/DMPC (1/1) (c) in buffer A at 24 °C. The corresponding phase diagram, which was roughly estimated from the measured area−pressure isotherms, is shown in the inset. As an example, the composition of an equimolar mixture consisting of 50% LE and LC phases is given.

labeled DNA−protein complexes are formed, migrating much slower in the gel (Figure 2a). Complex formation reaches saturation at a HSF24-to-DNA ratio of 2. Further addition of protein leads to a diffuse band due to multivalent interactions that shift the complexes to lower gel mobility. Complex formation is highly specific. In contrast to mutated dsHSE3 (Figure 2b,c) or 800 ng of salmon sperm DNA (not shown), unlabeled dsHSE3 effectively competes for DNA−protein complex formation (Figure 2b). Identical results were obtained with histidine-tagged and wild-type HSF24.

Chelator Lipid Layers as Specific Docking Interfaces. To achieve a lateral organization of the chelator lipids within the lipid monolayer, we spread an equimolar mixture of chelator lipid (Ni-NTA−DODA) and DMPC as matrix lipid. In Figure 3, the area−pressure isotherms demonstrate that the chelator lipid condenses at a drastic lower pressure (π_m = 10 mN/m at 24 °C) in comparison to DMPC (π_m = 40 mN/m at 24 °C) (Albrecht et al., 1978). The phase transition (LE/LC phase) of the equimolar mixture Ni-NTA−DODA/DMPC occurs in a pressure region in between, leading to a significant slope of the isotherm in the two-phase region (Figure 3c). The roughly estimated binary phase diagram exhibits a lenslike two-phase region (LE/LC) of an isomorphous system (inset of Figure 3). Applying standard thermodynamics, the composition of the phases can be estimated in the two-phase region (Cevc & Marsh, 1987). Given an equimolar mixture that consists of 50% LE and LC phase, the LC domains contain about 80 mol % of chelator lipid. In principle, the same situation holds true for mixtures with unloaded chelator lipid (NTA−DODA). Missing the complex ion that compensates repulsive negative charges of the NTA head group, the phase transition is shifted to higher pressures for NTA−DODA as previously analyzed (Schmitt et al., 1994; Dietrich et al., 1995). The lenslike form of the binary phase diagram is not changed, and estimated values for the concentration distribution for Ni-NTA−DODA and NTA−DODA are similar (not shown).

To study specific and unspecific protein binding to a laterally structured lipid layer, an equimolar mixture of chelator lipid and DMPC was spread on buffer A (T = 20 °C) which contained 0.5 nmol (15 nM) of fluorescence-labeled dsHSE3. To stain the fluid LE phase of the lipid monolayer, the lipid mixture was doped with fluorescence-labeled lipid (TR-DPPE, 0.1 mol %). Compression was

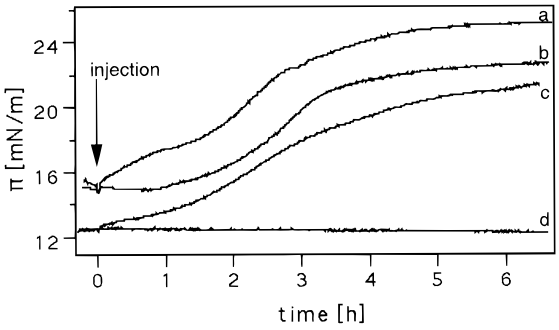

FIGURE 4: Protein interaction with lipid monolayers. An equimolar mixture of DMPC and loaded (Ni-NTA−DMPC) or unloaded (NTA−DODA) chelator lipid, respectively, was spread on buffer A supplemented with 0.5 nmol (15 nM) of oligonucleotide dsHSE3. After compression to 12−15 mN/m, the surface area of the monolayer was kept constant. Traces a−c show time-dependent changes of surface pressure after injection of 1.5 nmol of HSF24, yielding a final concentration of 45 nM. (a) Ni-NTA−DODA/DMPC monolayer, HSF24 with histidine tag. (b) NTA−DODA/DMPC monolayer, HSF24 with histidine tag. (c) Ni-NTA−DODA/DMPC monolayer, HSF24 without histidine tag. (d) Ni-NTA−DODA/DMPC monolayer, no protein injection.

performed to induce the formation of LC domains. The compression was stopped when about 50% of the area was covered with LC domains. At this point, the LC domains show still Brownian motion. As known from phospholipids [reviewed by McConnell (1991) and Möhwald (1990)], a long-range repulsive interaction prevents domain fusion and induces pattern formation and lateral order of the domains. The fluorescent oligonucleotide dissolved in the subphase is visible by a diffuse fluorescence image; it does not interact with the lipid monolayers used in the experiments.

The injection of 1.5 nmol of HSF24 to such preformed structured lipid films leads to significant changes. The effect on the lateral pressure is illustrated in Figure 4. Independent of the chelator lipid (nickel-loaded or unloaded state, Figure 4a,b) or of the added protein species (with or without histidine tag, Figure 4a,c), an increase of the surface pressure was observed. The related fluorescence micrographs of the lipid layers demonstrate that protein adsorption correlates with a loss of Brownian motion and a decrease of the lateral order of the domains. This is obviously due to the changes of the former fluid LE phase which exhibits a much higher viscosity, and a reduced diffusion as observed by photobleaching techniques. The size of the LC domains is hardly affected by the protein adsorption.

Immobilization via Histidine Tag and Chelator Lipid Restores Protein Function. DNA−protein complex formation was ensured by adding a 3-fold excess of HSF24 in relation to oligonucleotide to the subphase (see Figure 2). Therefore, the protein adsorption and the lateral distribution of functional DNA−protein complexes could be analyzed by epifluorescence microscopy. After pressure equilibration, fluorescence images of the oligonucleotide reveal drastic differences depending on the immobilization process. In the case of a nickel-loaded chelator lipid monolayer (Ni-NTA−DODA/DMPC, 1/1), addition of HSF24, subsequent complex formation, and binding to the lipid layer lead to a significant enrichment of the oligonucleotide at the LC domains (Figure 5). The pattern of the two micrographs is identical but inverse in contrast, demonstrating that functional DNA−HSF24 complexes are enriched at chelator lipid-rich domains possibly by a specific interaction of the histidine tag with the chelator lipid.

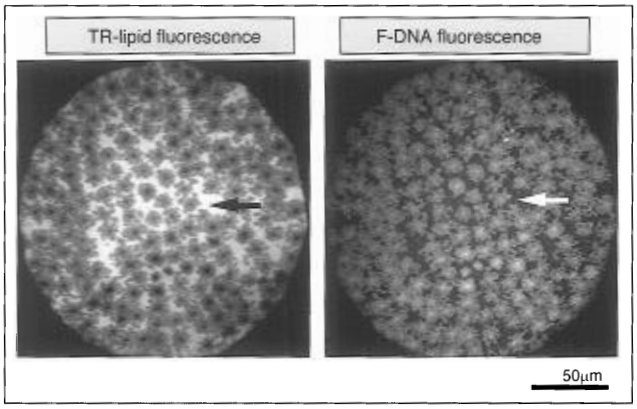

FIGURE 5: Epifluorescence microscopy. Fluorescence micrographs of a Ni-NTA−DODA/DMPC (1/1) lipid monolayer doped with 0.1% TexasRed lipid on subphase buffer A at 25 mN/m (20 °C). Buffer A was supplemented with 0.5 nmol (15 nM) of fluorescence-labeled oligonucleotide dsHSE3 FT/NB. Ten hours after injection of 1.5 nmol (45 nM) of histidine-tagged HSF24 into the subphase, the lateral distribution of TexasRed lipids staining the fluid phase (a, left panel) and DNA (b, right panel) was imaged by epifluorescence microscopy. Surface pressure change follows trace of panel a. Both pictures show identical structures but in an inverse contrast. Identical positions are marked by arrows.

To provide further evidence for a specific interaction, a lipid film containing the unloaded chelator lipid (NTA−DODA) was used. Although the protein interacts with the lipid layer as shown in Figure 4b, the oligonucleotide was not enriched at the lipid interface: Hence, no contrast of the DNA fluorescence was detected (Figure 6, top right). Note, the lipid fluorescence is still structured in chelator lipid-rich LC domains surrounded by the fluid phase. Addition of nickel ions, which induce complex formation of the chelator lipid head group, leads to a drastic change of the DNA fluorescence. Now, equivalent to the experiment with the preformed Ni-NTA−DODA/DMPC layer (Figure 5), DNA−protein complexes are enriched at the chelator lipid-rich domains. The fluorescence patterns of the lipid fluorescence (Figure 6, lower left) and DNA fluorescence (Figure 6, lower right) are identical but inverse in contrast. Injection of EDTA (0.5 mM final concentration) causes the disappearance of the oligomer fluorescence (not shown). As a further control, HSF24 without histidine tag was added to a structured nickel-loaded chelator lipid layer (Ni-NTA−DODA/DMPC, 1/1) identical to the monolayer described in Figure 5 (left panel) and Figure 6 (see time trace of Figure 4c). Although the chelator lipid is nickel-loaded, no enrichment of the oligonucleotide and no contrast in the DNA fluorescence were detected (not shown). In the absence of protein, the oligonucleotides do not interact with the lipid layer. This result is confirmed by surface pressure measurements and by epifluorescence micrographs at lipid monolayers in the absence of protein. Furthermore, the area−pressure isotherms of Ni-NTA−DODA, NTA−DODA, DMPC, and chelator lipid/DMPC monolayer are not affected by the oligonucleotide (not shown).

DISCUSSION

In solution, wild type as well as histidine-tagged HSF24 specifically recognizes DNA sequences that contain heat shock promotor elements (Figure 2). By contrast, at the lipid interface, HSF−DNA complex formation is directly depend-

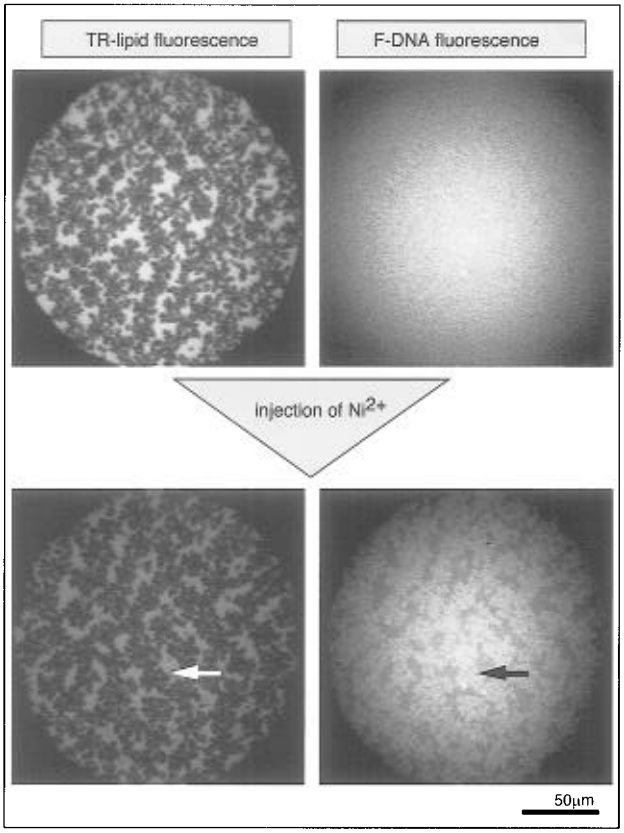

FIGURE 6: Fluorescence micrographs of a NTA−DODA/DMPC (1/1) monolayer doped with 0.1% TexasRed lipid on subphase buffer A at 23 mN/m (20 °C). The experimental procedure is given in detail in Figure 5. Ten hours after injection of histidine-tagged HSF24, the lateral distribution of TexasRed lipids (a, top left) and DNA was imaged (b, top right). Surface pressure change follows trace of Figure 5b. In contrast to Figure 5b, no contrast in the oligonucleotide fluorescence was detectable. This situation is drastically changed when nickel ions are injected. Three hours after addition of 3 μmol of $NiCl_2$ yielding a final concentration of 0.1 mM, the lipid fluorescence (c, bottom left) and the DNA fluorescence (d, bottom right) show identical patterns that are inverse in contrast. Identical positions are marked by arrows.

ent on the presence or absence of the histidine tag and chelator lipid. Two topics are essential for the understanding of this result:

(1) Protein adsorption to the lipid monolayer: The effects of the surface pressure as well as the altered properties of the lipid film indicate that, independent of a histidine tag attached to the protein and independent of the composition of the lipid layer, protein adsorption occurs. This can be explained by the fact that HSF24 (45 nM wild type or fusion protein) dissolved in buffer A is surface-active (equilibrium spreading pressure of 20 mN/m) while the protein was injected underneath a lipid monolayer at a pressure less than 15 mN/m. This *per se* promotes unspecific adsorption due to the interaction of the protein with the air−water interface.

(2) Function of the adsorbed protein: Due to the surface activity of HSF24 and the low surface pressure of the lipid layer, protein adsorption and denaturation orrur at the interface, which leads to the loss of DNA-binding capability. By contrast, the highly defined attachment via the histidine tag and chelator lipid maintains the functionality of the protein. Additionally, adsorption and dissorption of DNA−protein complexes can be triggered in a reversible fashion by adding Ni^{2+} or EDTA. The lateral distribution of the chelator lipid correlates with bound oligonucleotide and therefore with functional protein attached to the lipid layer. The only possible explanation is the enrichment of the chelator lipid in the LC domains as demonstrated by the binary phase diagram. This is confirmed by the observation that the DNA fluorescence is slightly increased in the center of the domains (Figure 5, right panel). Corresponding to the condensation process of the binary Ni-NTA−DODA/DMPC mixture and to the low lipid mobility in the LC phase which conserves lipid distribution for long times, the concentration of Ni-NTA−DODA in the domain center must be increased in comparison to the border of the domains. This correlates obviously with the increased DNA fluorescence and therefore with the increased adsorption of functional protein in the center of the domains. Docking of DNA−protein complexes is not induced by the phase condition of the lipids, since DNA−protein complexes without histidine tag are not bound. Histidine-taged DNA−protein complexes are only bound if complex formation of the chelator lipid is achieved.

The presented experiments demonstrate that the immobilization of histidine-tagged biomolecules to a membrane interface via coordinative binding to chelator lipids is a promising strategy to achieve a highly defined immobilization of these molecules to an interface maintaining their functional integrity even under conditions that promote protein denaturation at the interface. This result could be important for the preparation of biofunctionalized surfaces which allow various technical applications in biosensors or as biocompatible surfaces. An iminent advantage lies in the high generality of this noval binding concept which allows the application to various proteins to study molecular and cellular recognition processes at membranes.

ACKNOWLEDGMENT

The fruitful discussions and critical comments by Dr. Erich Sackmann (TU München, Garching), Dr. Lutz Nover (University Frankfurt), and Ingmar Dorn (TU München, Garching) are gratefully acknowledged.

REFERENCES

Adamson, A. W. (1990) *The physical chemistry of surfaces*, John Wiley & Sons, New York.

Albrecht, O., Gruler, H., & Sackmann, E. (1978) *J. Phys. (Paris) 39*, 301−313.

Cevc, G., & Marsh, D. (1987) *Phospholipid Bilayers*, John Wiley & Sons, New York.

Clos, J., Westwood, J. T., Becker, P. B., Wilson, S., Lambert, K., & Wu, C. (1990) *Cell 63*, 1085−1097.

Dietrich, C., & Tampé, R. (1995) *Biochim. Biophys. Acta* (in press).

Dietrich, C., Goldmann, W. H., Sackmann, E., & Isenberg G. (1993) *FEBS Lett. 324*, 37−40.

Dietrich, C., Schmitt, L., & Tampé, R. (1995) *Proc. Natl. Acad. Sci. U.S.A.* (in press).

Gains, G. L. (1966) *Insoluble monolayers at liquid-gas interfaces*, John Wiley & Sons, New York.

Graham, D. E., & Phillips, M. C. (1978) *J. Colloid Interface Sci. 70*, 427−439.

Gritsch, S., Neumaier, K., Schmitt, L., & Tampé, R. (1995) Biosens. Bioelectron. (in press).

Hochuli, E., Bannwarth, W., Döbeli, H., Gentz, R., & Stüber, D. (1988) *Bio/Technology 6*, 1321−1325.

Kühner, M., Tampé, R., & Sackmann, E. (1994) *Biophys. J. 67*, 217−226.

Laemmli, U. K. (1970) *Nature 227*, 680−685.

Lang, H., Duschl, C., Gratzer H., & Vogel H. (1992) *Thin Solid Films 210*, 818−821.
Lee, K. C., Klingler, J. F., & McConnell, H. M. (1994) *Science 263*, 655−658.
Martin, F. J., Hubbell, W. L., & Paphadjopoulos, D. (1981) *Biochemistry 20*, 4229−4238.
McConnell, H. M. (1991) *Annu. Rev. Phys. Chem. 42*, 171−195.
McRitchie, F. (1986) *Adv. Colloid Interface Sci. 25*, 341−385.
Möhwald, H. (1990) *Annu. Rev. Phys. Chem. 41*, 441−476.
Mulvihill, J. N., Schmitt, A., Maisonneuve, P., & Pusineri, C. (1985) *Colloids Surf. 14*, 317−325.
Norde, W. (1986) *Adv. Colloid Interface Sci. 25*, 267−340.
Nover, L. (1987) *Enzyme Microb. Technol. 9*, 130−144.
Nover, L. (1991) *Heat Shock Response*, CRC Press, Boca Raton, FL.
Nitsch, W., & Maksymiw, R. (1990) *Colloid Polym. Sci. 268*, 452−459.
Porath, J., Carlsson, J., Olsson, I., & Belfrage, G. (1975) *Nature 258*, 598−599.
Scharf, K.-D., Rose, S., Zott, W., Schöffl, F., & Nover, L. (1990) *EMBO J. 9*, 4495−4501.
Scharf, K.-D., Materna, T., Treuter, E., & Nover, L. (1994) in *Plant Promoters and Transcription Factors*, (Nover, L., Ed.) pp 121−158, Springer-Verlag, Berlin.
Schmidt, C. F., Zimmermann, R. M., & Gaub, H. E. (1990) *Biophys. J. 57*, 577−588.
Schmitt, L., Dietrich, L., & Tampé, R. (1994) *J. Am. Chem. Soc. 116*, 8485−8491.
Spinke, J., Yang, J., Wolf, H., Liley, M., Ringsdorf, H., & Knoll, W. (1992) *Biophys. J. 63*, 1667−1671.
Studier, F. W., Rosenberg, A. H., Dunn, J. J., & Dubendorff, J. W. (1990) *Methods Enzymol. 185*, 60−89.
Tamm, L., & McConnell, H. M. (1985) *Biophys. J. 47*, 105−113.
Tampé, R., Dietrich, C., Elender, G., Gritsch, S., & Schmitt, L. (1995) in *Nanofabrication and Biosystems: Integrating Materials Science, Engineering, and Biology* (Hoch, H. C., Jelinski, L., & Craighead, H., Eds.) Cambridge University Press, London (in press).
Treuter, E., Nover, L., Ohme, K., & Scharf, K.-D. (1993) *Mol. Gen. Genet. 240*, 113−125.
Tscharner, V., & McConnell, H. M. (1981) *Biophys. J. 36*, 421−427.
Ulman, A. (1991) *An introduction to ultrathin organic films*, Academic Press, San Diego.
Xiao, H., & Lis, J. T. (1988) *Science 239*, 1139−1149.
Zimarino, V., & Wu, C. (1987) *Nature 327*, 727−730.

BI952305+